JOURNAL OF THERMOPHYSICS AND HEAT TRANSFER
Vol. 13, No. 3, July–September 1999

Nucleate Pool Boiling over Vertical Steps

John Baker* and Krishna Prasad A. K.†
University of Alabama at Birmingham, Birmingham, Alabama 35294-4461

Nucleate subcooled pool boiling of water over vertical steps was carried out under atmospheric conditions. Two forward-facing steps of 0.8125 and 0.50 in. were considered. Data were statistically analyzed to determine sampling error. The ebullition was qualitatively explained in terms of thermal/flowfields and bubble dynamics. Plots of boiling heat flux vs superheat and surface heat transfer coefficient vs heat flux have been provided. Empirical correlations, developed from the above-mentioned data, are also presented. Boiling on vertically extended surfaces showed an increase in heat flux for a given superheat when compared with a plain vertical surface because of fluid agitation in the region of the step. The parameters associated with bubble dynamics and bubble interactions were also qualitatively discussed.

Nomenclature

C = correlation constant
h = surface heat transfer coefficient, kW/m^2 K
n = exponential constant
q = ebullition heat flux, kW/m^2
T = temperature, K

Subscripts

p = pool conditions
w = wall conditions

Introduction

HEAT transfer by means of phase change, i.e., boiling, is the most effective means of transferring energy in areas where a high rate of heat transfer needs to be achieved at near-isothermal conditions. Boiling by direct immersion techniques is increasingly used as an efficient form of heat transfer from high heat flux components such as electronic devices. The present trend is to enhance boiling by use of various surface modifications to achieve better operating efficiencies at lower operating costs.[1]

Although there is a wealth of literature in the area of nucleate boiling heat transfer,[2–4] it is seen that nucleate pool boiling on vertical cylindrical surfaces has not been investigated in its completeness. Further, boiling on vertically extended surfaces in the form of forward-facing steps has not been investigated before. Several researchers[5–10] have observed that nucleate boiling is more efficient when the surface is vertically oriented rather than in the horizontal position because of the varying nature of the thermal boundary layer and the buoyancy force, especially in the low heat flux region.[5] Boiling on downward-facing surfaces[7] was also found to be better than on upward-facing surfaces because of the differing nature of the thermal boundary layer, which is thicker for a downward-facing surface than for an upward-facing surface. To utilize completely the advantages of boiling by use of vertical plain and extended surfaces, a clear understanding of the process of nucleate boiling on these geometries needs to be achieved. The step can be considered as a downward-facing surface, and hence the extended surfaces considered here combine the advantages of both vertical and downward-facing surfaces. In this paper, the boiling mechanism has been qualitatively discussed and best-fit correlations based on a power-law-type regression have been obtained for the ebullition heat flux–superheat and heat transfer coefficient–heat flux variations. The variations in the parameters associated with a bubble are also discussed.

Received 24 November 1998; presented as Paper 99-0471 at the AIAA 37th Aerospace Sciences Meeting, Reno, NV, 11–14 January 1999; revision received 22 March 1999; accepted for publication 24 March 1999.

*Assistant Professor, Department of Materials and Mechanical Engineering. Member AIAA.
†Graduate Student, Department of Materials and Mechanical Engineering. Student Member AIAA.

Boiling Test Cell

Figure 1 presents a schematic diagram of the boiling test cell used in this investigation. The primary components of the test cell are a pool boiling tank, a heater/heat exchanger configuration capable of maintaining a constant pool temperature, a data acquisition/visualization system, and an instrumented cylindrical test specimen. The glass-walled pool boiling tank measured 300 mm in width, 480 mm in height, and 760 mm in length. The top of the tank was exposed to the atmospheric conditions. Energy was removed from the liquid within the pool boiling tank by two compact heat exchangers. The flow rate within each heat exchanger was controlled manually. Heat exchanger coolant (a mixture of ethylene glycol, diethylene glycol, and water) was circulated between the heat exchangers and a coolant reservoir by a submersible pump located within the coolant tank (not shown in the figure). In addition to the heat exchangers, two 2-kW submersion heaters were fixed within the pool boiling tank. The primary function of these heaters was to preheat the water within the tank. They were also used to maintain the temperature of the water in the tank when the energy from the heated test specimen was insufficient to offset heat losses from the pool boiling tank to the surroundings. Each submersion heater was regulated by a separate proportional–integral–derivative temperature/power controller. A data acquisition (DAQ) system recorded voltage readings from the 10 T-type thermocouples used to instrument the heated test specimen and the four T-type thermocouples used to measure the temperature of the water within the boiling tank. The DAQ system consisted of an external multiplexer board and a DAQ board mounted within a personal-computer-class computer (Pentium 90-MHz processor). An integrated-circuit temperature sensor, located on the multiplexer, was used for cold-junction compensation of the thermocouple readings. Thermocouple voltage readings were converted to temperature data by LabVIEW, a commercially available software package for DAQ, control, and analysis. Boiling behavior in the vicinity of the step was recorded by a digital video camera with a shutter speed of 1/4000 of a second and a 180 × digital zoom lens. Because of the quality of the video images obtained during the course of the investigation, no quantitative results were obtained.

Figure 2 is a schematic diagram of the cylindrical test specimen showing the dimensions of the thermcouples and the cartridge heater unit. The dimensions identified in Fig. 2 are specified for both step sizes in Table 1. The test specimen was mounted in the boiling tank vertically along the axis of the test specimen. The test specimen was formed from an aluminum (ASTMB221) rod. A forward-facing step was machined into the aluminum rod approximately halfway along the length of the rod with a step size of S, as indicated in Fig. 2.

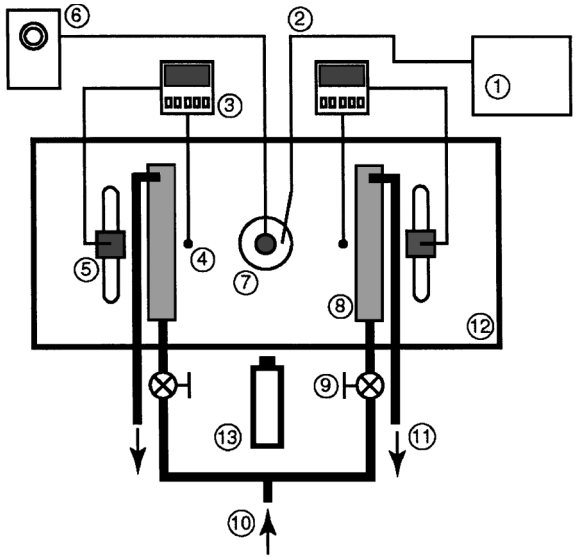

1. Computer/data acquisition system
2. Thermocouple wiring harness
3. Temperature/power controller
4. Thermocouple
5. Submersion heater
6. Variable power supply
7. Test specimen
8. Heat exchanger
9. Valve
10. Inlet from thermal reservoir
11. Outlet to thermal reservoir
12. Pool boiling tank
13. Digital camera

Fig. 1 Schematic representation of the experimental configuration.

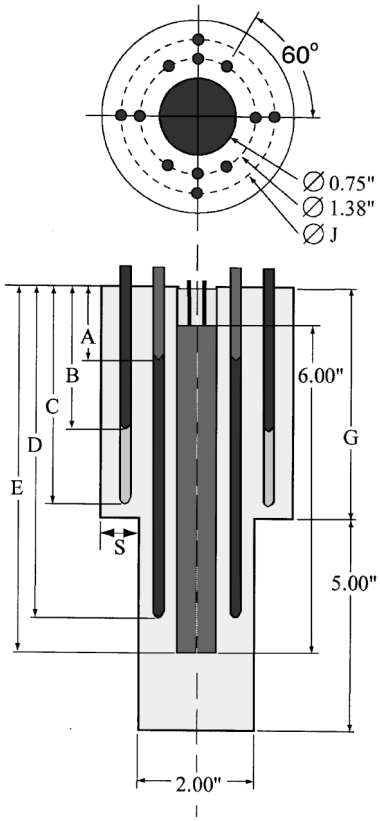

Fig. 2 Diagram of the test specimen.

Table 1 Dimensions[a] referenced in Fig. 2

Dimension	Case 1	Case 2
A	2.00	2.75
B	3.25	4.00
C	4.50	5.25
D	7.50	8.25
E	7.75	8.50
G	5.25	6.00
J	2.5	2.25
S	0.8125	0.500

[a] All measurements are in inches.

A hole (0.75-in. diam) was drilled to a depth E, as indicated in Fig. 2, to accommodate a cartridge heater unit. The cartridge heater (0.75-in. diam and 6.00 in. long) inserted into the test specimen had a power density rating of 0.25 W/mm^2 with a total wattage of 2 kW at 240 V. A variable power supply was used to regulate the power to the cartridge heater. The power supplied to the cartridge heater was determined with a voltmeter and an ammeter with uncertainties of ± 0.005 V and ± 0.005 A, respectively. Ten low-noise T-type thermocouples (4.75 mm in diameter) were located in the drilled thermocouple wells at five different depths in the test sections. Two thermocouples were positioned at each depth. The respective thermocouple well depths are indicated in Fig. 2 as dimensions A–D. The standard error for T-type thermocouples is reported as ± 1°C. Note that Fig. 2 is a schematic diagram, is not to scale, and should not be considered a mechanical drawing. Two cement-on bead-welded T-type thermocouples were located at the top of the test specimen to determine the temperature of that part of the test specimen outside the boiling pool. A heat transfer release coating fluid with a thermal conductivity approaching that of aluminum was used to fill completely any gaps that occurred between the cartridge heater and its corresponding mating hole in the test specimen because of machining tolerances. To minimize axial conduction losses, the space above the heater was filled with insulation and polystyrene foam. A surface-roughness estimate (root-mean-square value) was obtained with a Mitutoyo Surftest 402 instrument. This value was found to be 0.3 μm for both the test sections.

Experimental Procedure

All the trials were carried out at a water temperature of 90°C with atmospheric pressure at the upper pool surface. The statistical variation in the temperature at any two random depths of the pool was found to be less than 0.5°C before the onset of heating the test specimen. The test specimens were cleaned with acetone, dried, and then immersed into the boiling tank. The cartridge heater was then switched on. During each trial, the heat flux was varied accordingly to obtain a total of 16 heat flux steps with a final voltage of 240 V. Each heat flux step was maintained for at least 15 min to allow the boiling process to reach steady state. We verified steady-state conditions by noting the readings of the thermocouples located in the test sections and the pool boiling tank at regular intervals of time. The atmospheric pressure, thermocouple readings, and the input power to the cartridge heater were all recorded during each trial for future analysis.

The heat transferred to the liquid surrounding the test sections was computed after determination of the heat loss along the axial directions both above and below the heater, assuming one-dimensional heat conduction. The average heat loss that was due to axial conduction was observed to be of the order of 23% of the energy supplied to the cartridge heater, as determined from the voltage and current readings. This value represents the percentage lost for conditions under which the maximum power was being supplied to the cartridge heater. The surface temperature was computed after the resistance between the thermocouples and the outer surface of the test sections was accounted for by a one-dimensional radial heat conduction assumption. In the results presented in this paper, the impact of the existence of thermocouples in the test specimen and the associated heating of the electrical leads to the cartridge heater have been neglected.

Results and Discussion

The experiment involved subcooled nucleate pool boiling of water over vertically extended cylindrical surfaces, i.e., a vertical step under atmospheric conditions. The results are presented and discussed separately along two facets of the experiment:

1) the nature and the behavior of the temperature data from a statistical viewpoint

2) the boiling behavior as described by the plots and the qualitative analyses of the thermal and the hydrodynamic flowfields along with the nature of bubble behavior at various heat fluxes

The data set was composed of temperatures from the water in the boiling tank, temperatures from the test specimen, atmospheric-pressure measurements, and power measurements (voltage and current) from the cartridge heater.

Statistical Analysis

The data were examined to investigate the error associated with sampling. A detailed explanation is provided in Ref. 11. It was seen that once conditions of steady state had been reached, for a 95% confidence interval, 40 readings were a sufficient sample size for temperature measurements at each depth both from accuracy and time requirements. Confidence limits at a 95% confidence level were provided for the difference between means at each thermocouple location for each trial. The statistical error associated with measurement was provided in terms of the uncertainty associated in the measurement of the maximum heat flux value and it was equal to 0.1%. The F statistic was used for evaluating the number of trials. A two-factor analysis of variance (ANOVA) was carried out at each heat flux step size to determine if the variation in the thermocouple readings at each depth for several trials and the thermocouple readings at each trial for varying depths were due to randomness. The interaction between several trials and varying depths was also tested for randomness.

The confidence interval was given for the difference of means between the thermocouple readings at the same depth for different heat fluxes. The confidence interval matrix sampled for several heat fluxes during a single trial showed a uniform spread in value among all the cells. A test was also carried out to determine if the variation between the temperature values of the thermocouples at each depth was due to randomness alone. The results revealed that most of the time there was no statistical difference among the values. The probability of such a statistical difference at any heat flux for any pair of thermocouples located in the test section was found to be less than or equal to 0.1.

After the two-factor ANOVA was carried out at each heat flux step, it was seen that the variation in the thermocouple readings at each depth for several trials and the variation in the thermocouple readings at each trial for varying depths were because of randomness alone. The interaction between several trials and varying depths was also observed to be random.

Experimental Analysis

The ebullition heat flux, computed after the axial losses from the test specimen were accounted for, is plotted vs a modified superheat value in Fig. 3 for both step sizes. The modified superheat is defined as the difference between the wall temperature minus the boiling tank water temperature. Note that the definition of the modified superheat differs from the traditional definition of superheat, i.e., wall temperature minus saturation temperature. For subcooled boiling a term is also usually introduced to account for the fact that the pool is at a temperature less than saturation. Since the goal of this investigation is to determine the effect of the step and not to develop experimental correlations, the use of a modified superheat does not seem unreasonable. These plots presented in Fig. 3 represent the average of four trials chosen from among the many trials conducted. It should be noted that these four trials were picked on a random sample basis, although as a sequence, because the surface variability from trial to trial is an inherent occurrence. The calculated measurement uncertainty in the heat flux for both step sizes ranged from approximately ± 0.05 W at the minimum heat flux applied to approximately ± 1.2 W at the maximum heat flux value. The measurement uncertainty in the modified superheat value was calculated to be approximately ± 1.4°C. The above uncertainties are based on the accuracy of the measurement devices; they do not represent statistical uncertainty. From Fig. 3, it is seen that there are two distinct zones of heat transfer: a natural convection zone and a nucleate boiling heat transfer zone. The steep slope is characteristic of the boiling process wherein heat is removed both by sensible heat transport through the bubble and the latent heat transport of the microlayer beneath the bubble. The boiling heat transfer coefficient is also plotted against vs heat flux in Fig. 4, again based on the average of the four trial values. The measurement uncertainty in the boiling heat transfer coefficient for the 0.8125-in. step ranged from ± 0.0578 W/m^2 K at the minimum applied heat flux to ± 0.1498 W/m^2 K at the maximum applied heat flux. For the 0.5-in. step size, the measurement uncertainty range was from ± 0.0022 W/m^2 K at the minimum applied heat flux to ± 0.183 W/m^2 K at the maximum applied heat flux.

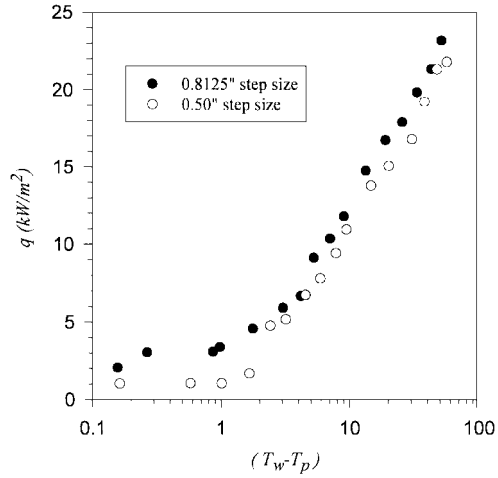

Fig. 3 Boiling heat flux vs modified superheat.

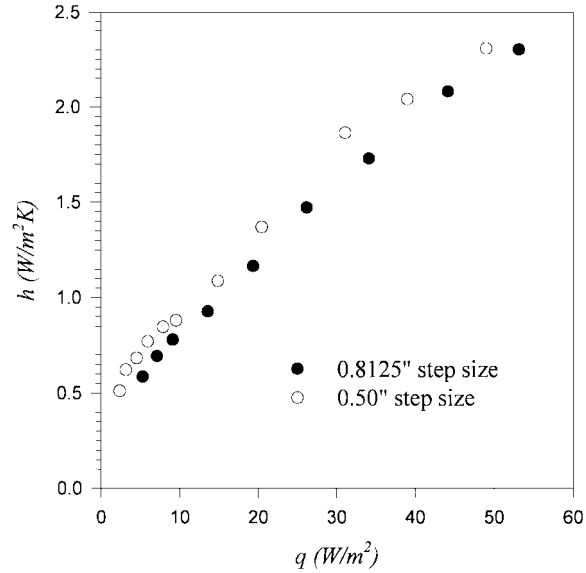

Fig. 4 Boiling convection coefficient vs boiling heat flux.

From the experimental data, correlations for the pool boiling heat transfer as functions of the modified superheat were obtained with power-law-type regression. Note that these correlations are not valid over the entire nucleate pool boiling regime for water at atmospheric pressure and are presented only to illustrate the impact of the step on boiling characteristics. Data were obtained up to a maximum wattage of 2 kW, which was insufficient to obtain critical heat flux conditions. The heat flux correlations are in the form of

$$q = C_1(T_s - T_w)^{n_1} \tag{1}$$

Table 2 Empirically determined constants and correlation coefficients for Eq. (1)

	Step size, in.	
Variable	0.8125	0.500
C_1	0.0207	0.0995
n_1	2.4771	2.0037
R^2	0.9870	0.9842

Table 3 Empirically determined constants and correlation coefficients for Eq. (2)

	Step size, in.	
Variable	0.8125	0.500
C_2	0.2057	0.3091
n_2	0.6016	0.5097
R^2	0.9942	0.9847

where the values of C_1, n_1, and the respective correlation coefficient R^2 are found in Table 2. Similarly, correlations for the convective heat transfer coefficient were obtained. These correlations are presented in the form of

$$h = C_2 q^{n_2} \tag{2}$$

where the values of C_2, n_2, and the respective correlation coefficients R^2 are found in Table 3. It was seen that the surface heat transfer coefficient for the vertical step of size 0.8125 in. was ~80% more than that for vertical plain cylinder results.[11] For the step size of 0.500 in., the heat transfer coefficient was nearly twice than that for a vertical plain cylinder.[11]

Three zones of boiling could be defined based on visualizing the process. These are below the step, the step itself, and above the step. Boiling in the region below the step was found to be vigorous with the production of a large number of bubbles. The nature of the bubble parameters was found to be similar to those of a plain vertical cylinder.[11] The thermal boundary-layer profile during the natural convection period showed a thickening of the layer as it approached the step, and in the region of the step there was rapid fluid agitation. Once boiling was vigorous at high heat fluxes, the agitation increased not only because of the step but also because of the formation of bubbles along the step. Contrary to the occurrence of a reattachment zone during natural convection of air over a step,[12] here the boundary layer developed at the outside edge of the step itself and progressed into the region above the step. It was seen that, because of the nature of the thermal and hydrodynamic boundary layers, the bubbles that originated from the region below the step tended to hit the step at points well inside of the inside edge of the step. This is also valid for the bubbles that originate from points well below the step region. However, for those bubbles that originated at lengths that were very close to the inside edge of the step, the nature of the bubble interaction had to be considered. The number of active nucleation sites was found to increase with an increase in heat flux.

The boiling heat transfer below the step was similar to that of a plain vertical cylindrical surface. After the video recordings were analyzed, it was seen that at a low heat flux (5.94 kW/m^2) there were certain active sites for bubble growth on the surface of the test section. The tendency of the bubbles to slide along the vertical surface (both below and above the step) was observed at low heat fluxes only. This sliding bubble implies the existence of a liquid layer between the bubble and the surface since the possibility of a fully grown bubble's sliding is not possible because of the flow of the surrounding liquid onto the surface behind the wake of the bubble that aids in its departure. Further, a fully grown or departing bubble does not have any interfacial contact with the surface that may be thought to be responsible for the slide.

The sliding nature of the bubbles above and below the step has been explained in detail by Prasad,[11] who used the three-phase-line (TPL) approach proposed by Mitrovic.[13] In Fig. 5, two interfaces in

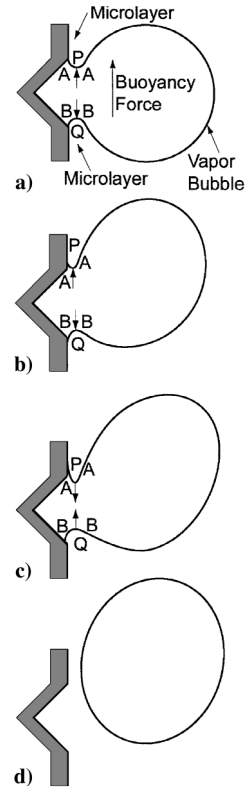

Fig. 5 Vapor bubble during a) initiation, b) growth, c) just before detachment, d) after detachment.

the microlayer region are defined for the growing vertical bubble. These are the leading (AA) and trailing (BB) interfaces. The TPL motion, as proposed by Mitrovic,[13] influences both AA and BB. During the bubble's growth, the directions of the interface motions are as shown in Fig. 5. It is seen that for interface AA, the direction of interface motion and the buoyancy vector are both in the same direction, whereas for the interface BB, the directions are reversed. This implies that the rates of motion of interfaces AA and BB are different. This difference is believed to be the cause for bubble's sliding. The slide can be considered to be a result of the interfacial–interfacial motion that exists between AA and BB.

During departure it is seen that the motions of AA and BB are reversed and are toward the cavity mouth. This causes interface BB to move at a higher rate compared with that of AA. This may cause interface BB to slide into the cavity at which it originated. Finally the two interfaces meet each other, after which the bubble departs. The flow of liquid into the microlayer is also to be considered along with the forces and heat transfer effects in explaining the interfacial motions. As interface AA moves up during growth, there is also a continuous latent heat transfer across the microlayer. This causes the interface to grow as it moves. Because interface AA moves at a rate higher than that of BB, the heat transfer through the microlayer is not uniform for both interfaces AA and BB. For the bubble to grow rather than collapse, the increase in motion of interface AA has to be compensated for by an additional amount of heat flow through microlayer P. This is because an interface motion away from the originating cavity causes an interaction with liquid, which is at a lower temperature than in the microlayer, and hence there is a possibility of heat transfer in the reverse sense, that is, from the bubble to the surrounding liquid. To circumvent this, heat transfer through microlayer P must be greater than that of microlayer Q.

Hence the sliding nature of the bubble depends on the interactions of the fluid thermal–mechanical parameters that vary both in time and space and also surface parameters like orientation and surface finish. Although the motion of interfaces AA and BB may be observed on a surface at all inclinations, it is unlikely that there will be an interfacial–interfacial motion observed on a horizontal upward-facing surface that is due to the nature of the buoyancy force.

However, the sliding nature of the TPL, as suggested by Mitrovic,[13] will in all probability occur. The surface finish relates on a microscopic scale to the number of active nucleation sites present and the bubble during its slide may activate sites that were initially dormant, thereby causing an increase in nucleation site density, which on a macroscopic scale affects the overall ebullition heat flux.

The bubble parameters and bubble behavior along the step are quite different from the rest of the test section. The step may be considered as a horizontal downward-facing surface (that is, heated from above). However, here the heat transfer is not uniform over the region of the step. This is due to the design and the construction of the test section that uses a single cartridge heater that is located at the center of the test section. This nonuniformity of heat flux transferred to the step influences the variation of bubble parameters on the outside of the step that, on a macrolevel, influences the ebullition heat transfer. The temperature at the inside edge of the step is found to be in excess of the temperatures recorded at the outside edge of the step by approximately 6% at maximum heat flux.

At low heat fluxes, it is seen that boiling first occurs around the inside edge of the step. The bubbles that originate are small in diameter and have a very low release frequency. These bubbles tend to slide along the step, and, in doing so, they may perform two functions that aid the ebullition process. Each bubble during its slide may uncover and activate additional nucleation sites, thereby causing vapor production to increase. The bubble during its transit along the step may also receive extra heat transfer from the microlayer that is beneath the bubble, causing the sum total of latent and sensible heat carried away per bubble to increase. However, these two functions are dependent on several factors, such as the nature of the bubble when it originates, the temperature gradient profile along the step, the nature of the surface, and the liquid temperature.

At moderate heat fluxes, the bubble formation is spread along the step, and the size of the bubbles (on an individual basis) is found to decrease as the distance from the inside edge to the outside edge of the step increases. The bubbles now tend to merge as they travel along the step. Again, Fig. 5 shows a schematic sketch of the behavior of bubbles on the surface. This has been drawn based on visual observations of the boiling process. This bubble merging causes the above-mentioned two functions to occur that accentuate the boiling process.

To explain the behavior described above, one may define a new parameter referred to as a bubble interaction parameter (BIP). This stochastic measure may vary from one to any positive number. If the BIP is equal to one, then it means that there is no bubble interaction and each bubble's history has no influence on or is influenced by other bubbles. The BIP is a stochastic measure, and hence one can speak of a range of values for the BIP for a specified confidence level. It is important at this point to differentiate between the BIP and the other usual parameters that are associated with a bubble. Note that the BIP makes sense only when more than one bubble is considered and that it is associated when a modified surface (step) only is considered. Hence it is not a parameter associated with a single bubble and a plain surface. BIP values indicate the coalescing nature of the bubbles. As mentioned above, at moderate heat fluxes the bubbles that form at the inside edge of the step tend to slide along the step, and in doing so they coalesce with other bubbles along the way until they reach the outside edge of the step. During this process the bubbles tend to grow in size and they acquire an elongated ellipsoidal shape. The shape depends on the step size. It is seen that the bubbles tend to have an intermittent, and not a smooth, motion during their transit toward the outside edge of the step. This may be because of the motion of the microlayer beneath the bubble and the corresponding pumping of heat energy into the growing bubble. (Note that here "growing" is used in the context of an increase in size caused by the merger of several bubbles.) It is known that even in the case of a single bubble on a plain surface, there is an area over which the bubble influences the behavior of nucleation sites.[14] Hence this also needs to be considered apart from the BIP measure when bubble interactions are analyzed in the step region.

Once the bubble reaches the tip (or outside edge) of the step, it moves up and condenses in the bulk liquid because the boiling is under subcooled conditions. At high heat fluxes, the frequency of bubble generation increases at the expense of its size, and the interaction of bubbles needs to be looked at from two points of view. As mentioned above, a greater percentage of the bubbles that originate from the region below the step hit the step at points well within the inside edge of the step. Hence these bubbles agitate the fluid and also interact with the bubbles along the step to enhance the heat transfer process. The vapor bubbles impinging on the step may also collapse or combine with bubbles formed at the step, although the probability of the latter is not great, as observed during the experiment. Nevertheless, this indicates that we have to consider BIP values from this viewpoint too.

Boiling in the region above the step is found to be smaller compared with that in the previous two zones. This may be due to the increased thickness of the test section (and hence an increase in resistance of heat transfer to the liquid) in the region above the step. It is seen that, because the bubbles that are formed at the step condense once they move out from the outside edge of the step, the bubbles in the region above the step undergo no interaction with the bubbles from the previous two zones. Further, even at high heat fluxes, the bubbles from this zone are not as large as those from the region below the step, nor is their frequency. This implies that the contribution of boiling in the region above the step to the overall boiling heat transfer is quite small.

The reduction of the step size from 0.8125 to 0.500 in. is found to influence the final size of the coalesced bubble as it departs from the outside edge of the step. It is seen that the final size of the bubble is smaller compared with a step size of 0.8125 in. However, ebullition heat transfer is better here than for the step size of 0.8125 in., and this may be due to the increased frequency of bubble generation that more than offsets the reduction of bubble size. It is seen that for the same heat flux, the surface heat transfer coefficient for a step size of 0.500 in. is in excess of the value for a step size of 0.8125 in. by $\sim$12%. Further, boiling in the region above the step size of 0.500 in. is found to be better compared with that of the 0.8125-in. step.

Conclusions

Pool boiling on vertical plain and extended surfaces under subcooled conditions in water at atmospheric pressure was performed. The vertically extended surfaces were in the form of forward-facing steps. A thorough statistical analysis was carried on the data, and the corresponding confidence interval and statistical variation matrices were determined. The boiling process was qualitatively described with the help of visual recordings and still image capture by a digital video camera. Best-fit correlation equations were obtained that relate the ebullition heat flux to superheat and the surface heat transfer coefficient to the ebullition heat flux. The influence of the step on enhancing the boiling process was described. The coupling of the sensible heat transfer and the latent energy transport on the extended surfaces was found to improve the heat transferred for the same degree of superheat. The aspect of sliding bubbles that was noted on all the vertical surfaces during experimentation was also explained.

It was seen that the sliding of the bubbles at low heat fluxes might be because of the interfacial–interfacial motion of the interface at the base of the bubbles. Among other parameters, the buoyancy force vector orientation determines the sliding. A qualitative explanation was provided that explains the nature of the interface motion and the fluid-thermodynamic effects associated with it. Boiling on the stepped surfaces was discussed with reference to the nature of the bubbles and their parameters. It was proposed that a new term, called the *bubble interaction parameter*, be defined that explains the extent of the coalescing nature of the bubbles along the step.

References

[1] Bergles, A. E., "Enhancement of Pool Boiling," *International Journal of Refrigeration,* Vol. 20, No. 8, 1997, pp. 545–551.

[2] Dhir, V. K., "Boiling Heat Transfer," *Annual Review of Fluid Mechanics,* Vol. 30, 1998, pp. 365–401.

[3] Fujita, Y., "The State of Art-Nucleate Pool Boiling Mechanism," *Engineering Foundation Conference on Pool and External Flow Boiling,* American Society of Mechanical Engineers, New York, 1992, pp. 83–97.

[4]Carey, V. P., *Liquid Vapor Phase Change Phenomena*, Hemisphere, Washington, DC, 1992.

[5]Lee, C. C., Chuah, Y. K., Lu, D. C., and Chao, D. Y., "Experimental Investigation of Pool Boiling of Lithium Bromide Solution on a Vertical Tube Under Subatmospheric Conditions," *International Communications in Heat and Mass Transfer,* Vol. 18, No. 3, 1991, pp. 309–320.

[6]Cho, C. S. K., Hwang, Q. N., Reddy, R. K., and Ayub, Z. H., "Enhanced Nucleate Boiling on Structured Surfaces," *Proceedings of the IEEE InterSociety Conference on Thermal Phenomena,* Inst. of Electrical and Electronics Engineers, New York, 1992, pp. 116–121.

[7]Nishikawa, K., Fujita, Y., Uchida, S., and Ohta, H., "Effect of Surface Orientation on Nucleate Boiling Heat Transfer," *International Journal of Heat and Mass Transfer,* Vol. 27, No. 9, 1984, pp. 1559–1571.

[8]Guo, Z., and El-Genk, M., "An Experimental Study of Saturated Pool Boiling from Downward Facing and Inclined Surfaces," *International Journal of Heat and Mass Transfer,* Vol. 35, No. 9, 1992, pp. 2109–2117.

[9]El-Genk, M., "A Review of Pool Boiling from Inclined and Downward Facing Flat Surfaces," *Heat and Technology,* Vol. 14, No. 2, 1996, pp. 95–104.

[10]El-Genk, M., and Guo, Z., "Saturated and Sub-Cooled Pool Boiling from Downward Facing and Inclined Surfaces," *The Engineering Foundation Conference on Pool and External Flow Boiling,* American Society of Mechanical Engineers, New York, 1992, pp. 243–259.

[11]Prasad A. K., K., "Experimental Investigation of Nucleate Pool Boiling over Vertical Extended Surfaces," M.S. Thesis, Univ. of Alabama, Birmingham, AL, Sept. 1998.

[12]Abu Mulaweh, H. I., Armaly, B. F., and Chen, T. S., "Laminar Convection Flow over a Vertical Backward Facing Step," *Journal of Heat Transfer,* Vol. 117, 1995, pp. 895–901.

[13]Mitrovic, J., "The Flow and Heat Transfer in the Wedge-Shaped Liquid Film Formed During the Growth of A Vapor Bubble," *International Journal of Heat and Mass Transfer,* Vol. 41, No. 12, 1998, pp. 1771–1785.

[14]Kenning, D. B. R., and Yan, Y., "Pool Boiling on a Thin Plate: Features Revealed by Liquid Crystal Thermography," *International Journal of Heat and Mass Transfer,* Vol. 39, No. 15, 1996, pp. 3117–3137.